

OFFSHORE NATURAL GAS PIPELINES SUBJECTED TO KINEMATIC DISTRESS

Dionysios N. Chatzidakis¹, Yiannis Tsompanakis^{1*}, Prodromos N. Psarropoulos²

¹ Technical University of Crete
Chania, Greece
*e-mail: jt@science.tuc.gr

² National Technical University of Athens
Athens, Greece

Keywords: Natural gas, offshore pipelines, geohazards, submarine landslides, mitigation measures, numerical simulations.

Abstract. *Hydrocarbons are undoubtedly the main energy source of the twenty-first century. Over the last decades the increase in energy needs has led to the exploitation of an increasing number of offshore natural gas deposits. Typically, the long distances between natural gas deposits and urban and industrial centres necessitate the use of offshore pipelines. Such pipelines are very important infrastructures and any possible damage can cause serious problems and devastating consequences. Geohazards, such as strong ground motion, active faults, tsunamis, etc, consist crucial threats that an offshore pipeline has to overcome. Especially, kinematic distress caused by active faults or submarine landslides can impose a great risk to offshore pipelines due to the substantial permanent ground deformations. Furthermore, the extended areas that are affected by such phenomena, as well as the adverse submarine soil conditions, are also detrimental factors for the integrity of the pipelines.*

For this purpose, the aim of this work is to study numerically, utilizing the finite element method, the kinematic distress) of an offshore natural gas pipeline due to a submarine landslide. Firstly, the developed numerical models are validated using available analytical solutions, and subsequently various parameters that affect the examined problem are investigated. The detailed parametric analysis covers among others, the impacted force on the pipeline, the landslide length, internal pressure levels, slope inclinations and diameter to thickness ratios.

1 INTRODUCTION

The increasing use of pipelines for transporting hydrocarbons (oil and natural gas) in recent decades has prompted several researchers to investigate the response of them under various loading conditions related to geohazards and other hazards. International or national standards and regulations, such as the American Lifeline Alliance (ALA), Eurocode 8, ISO 19900–19906 and DNVGL are the outcome of this work. Nevertheless, the majority of the international research and standards focus on the case of onshore pipelines, despite the fact that the use of offshore pipelines constantly increases. Kinematic distress due to geohazards (e.g., fault rupture, landslides, tsunamis, etc) is a crucial threat for offshore pipelines considering the long distances covered. Especially in deep waters, offshore pipelines are usually laid directly on the seabed surface which makes them vulnerable to the debris flow due to offshore landslides.

The investigation of offshore pipelines subjected to landslides could be divided into three parts: (a) the impact force assessment, (b) the pipe-soil interaction determination, and (c) the pipeline response assessment through experimental, analytical and numerical models. Considering the impact force assessment of a submarine landslide on an offshore pipeline a quite recent literature review [1] presents two approaches: the geotechnical and the hydrodynamic method. Zakeri et al. [2, 3], taking into account experimental data, derived analytical expressions for calculating the drag force on the pipelines depending on the soil conditions, the slope angle, the intersection angle, etc. Subsequently, Randolph & White [4] and Liu et al. [5] improved initial flaws of the analytical formulas taking into account additional parameters, while Sahdi et al. [6] investigated the problem via centrifuge experimental models.

Regarding the offshore pipeline soil interaction, the work of Bruton et al. [7] and White & Cheuk [8] are worth mentioning, since they investigated the axial and lateral pipe-soil interaction based on experimental modeling. Randolph et al. [9] and Wang & Yang [10] dealt with pipe-soil interaction, while Guha et al. [11] investigated more thoroughly the pipe-soil interaction, taking into account both the horizontal and vertical directions.

With respect to the pipeline response assessment, Parker et al. [12], Yuan et al. [13, 14], Yuan et al. [15] and Zhang et al. [16] present both analytical and numerical models, that investigate the case of landslide impact vertical to the pipeline axis. The landslide impact is simulated as a linear drag force and pipe-soil interaction is modeled through bilinear elastic-plastic springs. The pipeline non-linear response is not taken into account in of the aforementioned studies and the elastic beam theory of Euler-Bernoulli is adopted for the simulation of the pipeline.

Additionally, regarding the potential mitigation measures, quite recently Chatzidakis et al. [17] examined numerically whether the use of a double curvature would be beneficial for an onshore pipeline subjected to landslide along its axis and showed that for certain conditions this configuration could be advantageous.

The main objective of the current work is to investigate numerically the kinematic distress of a surface laid offshore pipeline subjected to a landslide impact vertical to its axis. For this purpose, firstly the proposed numerical model is verified with the results of the analytical and numerical models created by Yuan et al. [15]. Consequently, an extended parametric investigation is conducted focusing on the most significant parameters, such as landslide width and magnitude, internal pressure, cross section geometry, slope inclination, etc. The pipeline and soil properties used in compliance with the Mediterranean region characteristics, and specifically those used for the design of the offshore part of Trans Adriatic Pipeline (TAP) that connects Albania and Italy through Adriatic Sea.

2 PROBLEM AND MODEL DEFINITION

In this work, the problem of landslide impact in the middle of a 3 km long submarine natural gas pipeline vertical to its axis is considered, as shown in Figure 1. The pipeline is located between two fixed points, which could be for instance, wellheads, manifolds, anchors, etc. The impact forces due to the landslide can be calculated using geotechnical or hydrodynamic methods [5]. The calculation of the landslide forces is out of the scope of this work, therefore, the landslide impact is considered through a uniform linear force, q , in the middle of the pipeline.

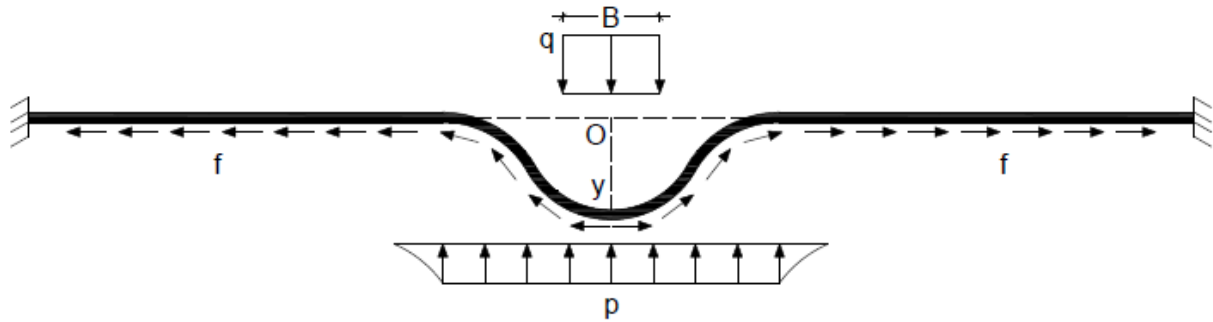


Figure 1: Pipeline configuration.

As shown in Figure 1, the lateral, p , and axial, f , pipe-soil interaction forces are considered, while the vertical pipe-soil interaction is not taken into account. The calculation of the pipe-soil interaction forces and relative displacements is also out of the scope of this work, and therefore, an elastic perfect-plastic behavior is considered for both lateral and axial directions. Figure 2 depicts the pipe-soil interaction pattern considered for the lateral and axial resistance. The maximum pipe-soil interaction force, p_0 , is mobilized for a pipe-soil relative displacement $0.1D$ on both directions. Respectively, the maximum axial pipe-soil interaction force, f_0 , is mobilized for an axial pipe-soil relative displacement equal to 5 mm on both directions. The above patterns are taken from [15], since this model is used herein to validate the examined model as described in the sequence.

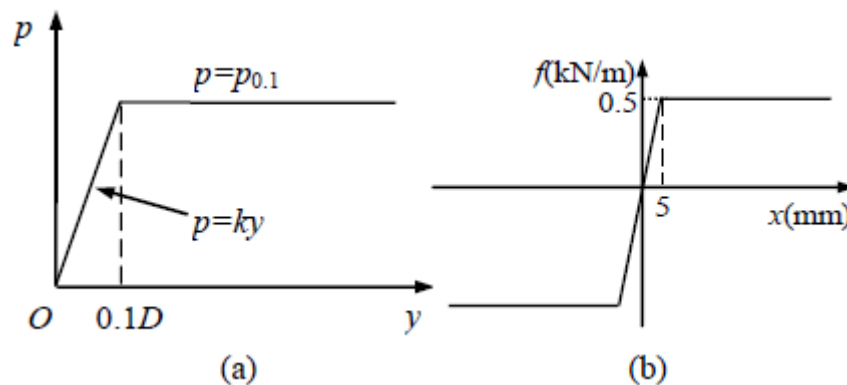


Figure 2: Pipeline-soil interaction for: (a) lateral and (b) axial direction.

The problem is modeled numerically utilizing the finite element method (FEM), using ABAQUS software [18]. The numerical model is divided into three parts according to the loading conditions and the proximity to the landslide. The first part is the pipeline length within the landslide area, in which the element length is equal to 0.5 m. The drag force due to

the landslide is considered uniform along the landslide area and both axial and lateral soil reactions are taken into account. The second part is on both sides of the landslide area up to 1000m from the center of the landslide. Due to the proximity to the landslide area, this part is modeled with 0.5 m elements and both axial and lateral soil reactions are taken into account. The third part is the last 1000 m of the pipeline on both sides up to the fixed ends. This part is modeled with 2 m elements and both axial and lateral soil reactions are taken into account, although the lateral soil reaction is very small.

The pipeline is modeled by Timoshenko beam elements using the pipeline element PIPE21 of ABAQUS. As shown in Figure 3, these elements have one integration point on the axial direction and four along the cross section. The pipeline configuration enables the implementation of both internal and external pressures in order to represent the gas and hydrostatic pressure, respectively. Considering the soil resistance, pipe-soil interaction elements (PSI24) are used to represent both lateral and axial soil resistances. These are four-node plain elements with two of them attached on the pipe and two representing the far field conditions, which are considered as fixed in this study. The axial interaction force is always parallel to the pipeline attached nodes. Large displacements, nonlinear plastic strains and geometrical nonlinear response are taken into consideration in a computationally efficient manner.

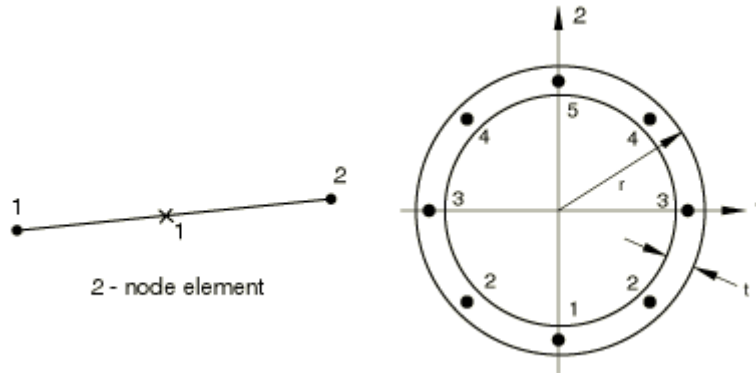


Figure 3: PIPE21 element integration points along the element and around the pipeline perimeter.

3 VALIDATION AND COMPARISON

To validate the numerical model proposed herein, the model is compared with the analytical and numerical approach of Yuan et al. [15]. The analytical approach is a result of the Euler-Bernoulli beam theory implementation in different segments of the pipeline depending on the loading conditions. Subsequently, the unknown parameters are obtained by implementing the known boundary conditions. It is noted that the axial friction is neglected in the segments where the lateral soil resistance is non-zero and that, although the axial tension varies along the pipeline, the horizontal component of the tension is considered constant.

The numerical approach is a result of the vector form intrinsic finite element method (VFIFE) implementation introduced by Ting et al. [19]. The pipeline is discretized into a series of nodes and elements, with the mass of the pipeline concentrated on the nodes. The pipeline movement is discretized into a series of small time steps, dt , with small deformations and constant material and dimensions in each step.

In order to compare the results of the proposed model with the aforementioned results, the pipeline properties and loading conditions used are the same as those used in [15]. Table 1 lists all the parameters used for the analysis, where D_{out} and D_{in} are the outer and internal diameters, respectively; B is the landslide width; q is the drag force impacted on the pipeline; p_0

and f_0 are the maximum lateral and axial soil resistance forces, E is the elastic modulus, and ν is the Poisson's ratio. It is noted that the pipeline is considered to have only elastic response.

Parameter	Value
D_{out} (m)	0.6
D_{in} (m)	0.55
q (kN/m)	6
P_0 (kN/m)	3
f_0 (kN/m)	0.5
E (GPa)	210
ν (-)	0.3

Table 1: Summary of parameters used for the validation.

As illustrated in Figure 4, the pipeline displacement obtained by all three approaches is similar, considering both the maximum pipeline displacement and the displacement configuration along the pipeline. It is noted that the maximum displacements of the two numerical models are almost identical and only slightly different from the analytical approach results.

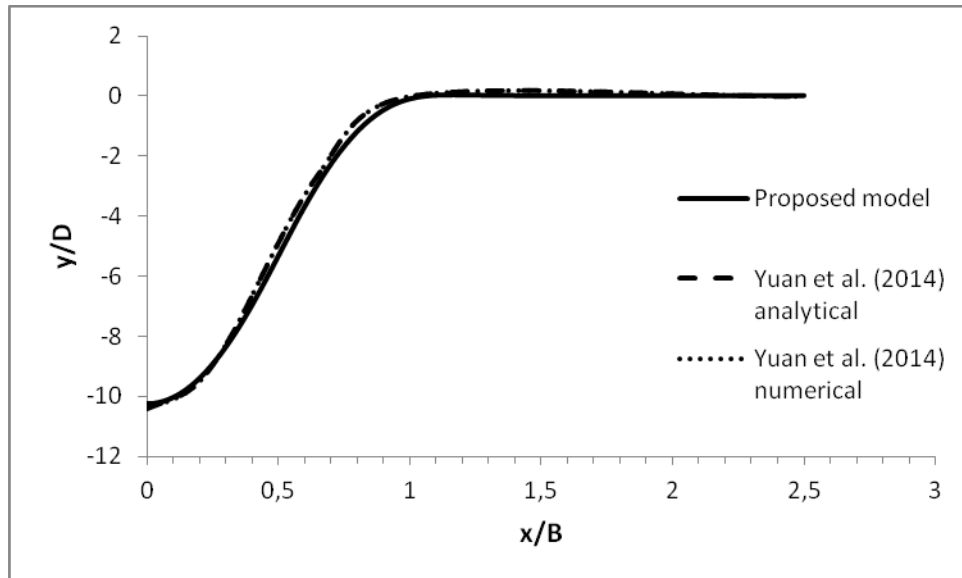


Figure 4: Comparison between normalized pipeline displacements.

On the other hand, greater discrepancies are observed between all three approaches considering the axial tension, as shown in Figure 5. The axial tension of the analytical model remains constant along the entire length of the pipeline because the axial soil resistance is not taken into account, while on both numerical models the axial tension is less almost from the middle of the landslide region. The axial tension in the middle of the examined configuration for the numerical model of Yuan et al. [15] is slightly different from the other two approaches which give similar results. However, the axial tension at greater distances from the middle of the examined geometry is smaller than for the other two models, which tend to converge to same values. Finally, the small increase of the axial tension observed in the numerical model of [15], does not occur in the proposed model.

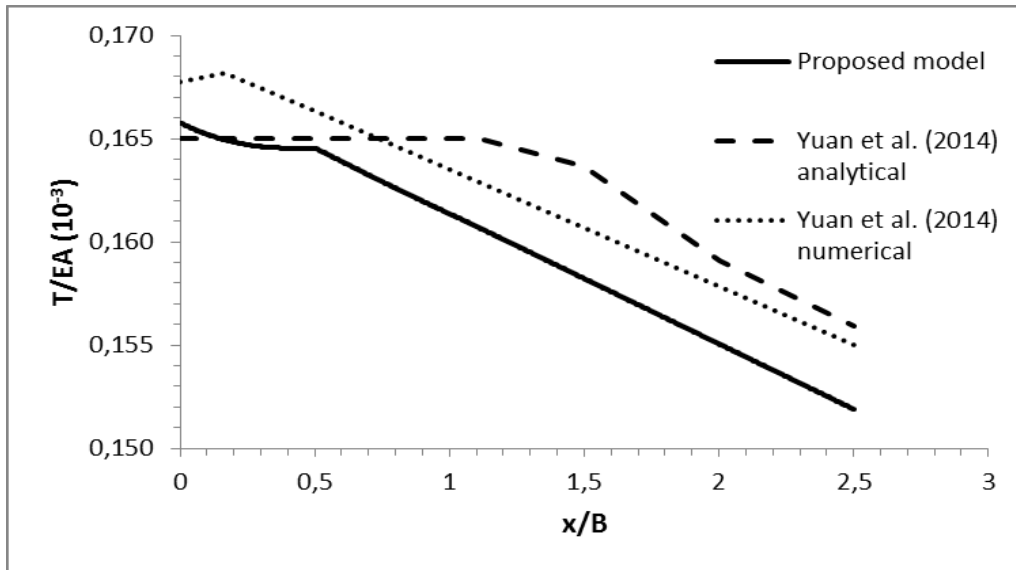


Figure 5: Comparison between normalized pipeline axial forces.

4 PARAMETRIC STUDY

In order to investigate the influence of various parameters on the pipeline response due to a severe landslide, a parametric study is conducted. The pipeline characteristics used for this study comply with the offshore section characteristics of TAP pipeline [20]. TAP is an under construction large-scale pipeline which crosses the seismically active Adriatic Sea and it is prone to submarine landslides. The parameters used for the base model are listed in Table 2, where B is the landslide width, t is the pipeline thickness, F_y is the yield stress for the X60 steel grade, ϕ is the bottom inclination, P_{in} is the internal pressure of natural gas, and P_{ext} is the external hydrostatic pressure of water depth of about 200 m. The total length of the pipeline, the boundary conditions, and the numerical model details used for the analysis are the same as mentioned previously for the benchmark case study [15].

Parameter	Value
B (m)	240
D_{out} (m)	0.9144
D/t	30
q (kN/m)	25
P_0 (kN/m)	5
f_0 (kN/m)	1.5
E (GPa)	210
ν (-)	0.3
F_y (MPa)	414
ϕ ($^\circ$)	0
P_{in} (kPa)	15000
P_{ext} (kPa)	2000

Table 2: Summary of parameters used for the parametric study.

4.1 Landslide drag force

Considering the landslide drag force influence on the pipeline, three different forces are used: $q = 5, 10$ and 25 kN/m. In all cases the drag force is uniform along the pipeline in the

landslide area. As shown in Figure 6, larger drag force results in larger lateral normalized displacements, y/D , while a longer part of the pipeline moving laterally. It can be noticed that the absolute lateral movement of the pipeline is large in every case, and more specifically 3.77, 14.19 and 38.72 m for 5, 10 and 25 kN/m drag force, respectively. Moreover, the length of the pipeline moving laterally is 135, 216 and 552 m, for 5, 10 and 25 kN/m drag force values, respectively.

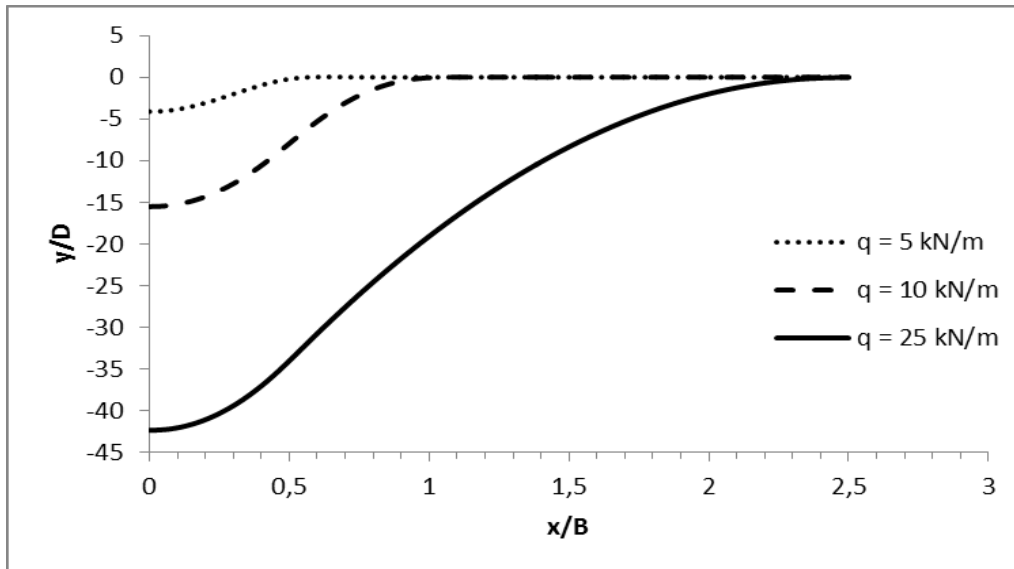


Figure 6: Comparison between normalized pipeline displacements for different drag forces.

Pipeline failure is a complex phenomenon which usually is considered in terms of strains instead of stresses [21]. The fact that steel is the most commonly used material explains the above assumption. Additionally, lateral movement of the pipeline created bending deformation on various points along the pipeline. Therefore, the axial strain, ε_{11} , on both the bottom (point 1 of Figure 3) and the top line (point 5 of Figure 3) of the pipeline cross section is used to investigate the possibility of pipeline failure for every case.

As shown in Figure 7, the bottom line strains receive maximum values in the middle of the pipe and minimum after the landslide area, while the top line strains display the reverse pattern. In the case of $q = 25$ kN/m, both top and bottom strains are tensile and match just after the landslide ($x/B = 0.5$). In the case of $q = 10$ kN/m, both bottom and top strains display a minimum and maximum, respectively at a normalized distance $x/B = 0.75$ after the landslide. Finally, in the case of $q = 5$ kN/m, both bottom and top strains display a minimum and maximum, respectively at the end of the landslide and compressive strains appear at both the middle of the pipe and the end of the landslide. It is emphasized that for thin steel pipelines compressive strains are more critical than tensile strains due to the potential occurrence of local buckling phenomena.

4.2 Landslide width

Regarding the influence of the landslide width on the pipeline, three different widths have been examined: $B = 60$, 120 and 240 m. As presented in Figure 8, greater width results in larger lateral normalized displacements, y/D , while the part of the pipeline moving laterally remains constant. The absolute lateral movement of the pipeline is large in every case, and more specifically 10.37, 19.91 and 38.72 m for 60, 120 and 240 m width, respectively. In addition, the length of the pipeline moving laterally is 552 m in all cases.

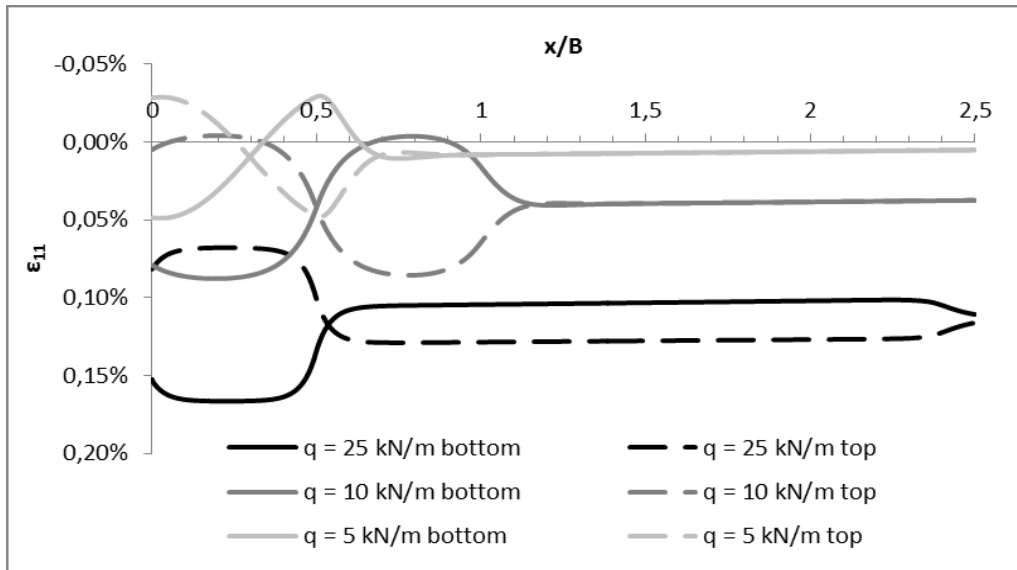


Figure 7: Comparison between axial strains for different drag forces.

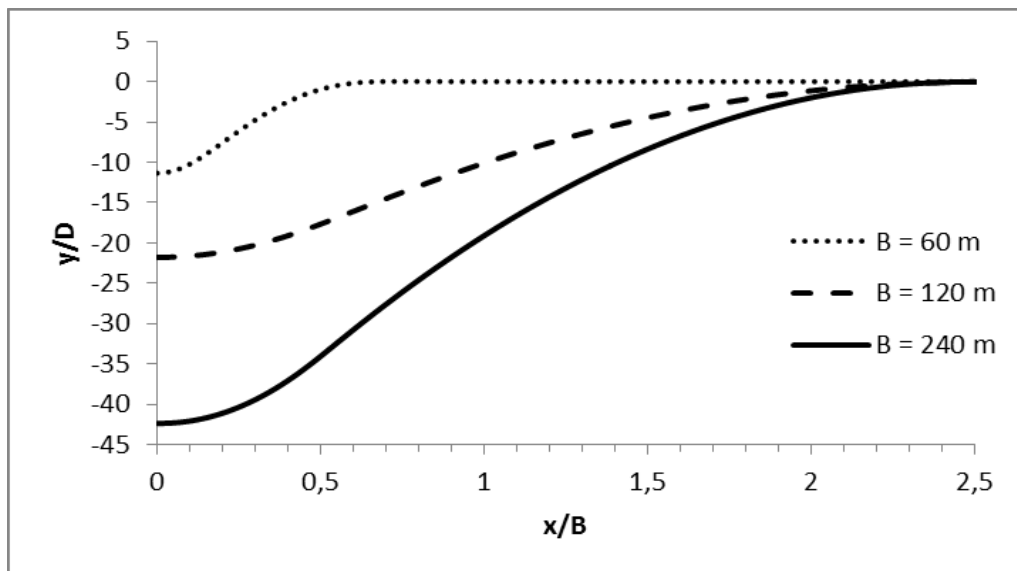


Figure 8: Comparison between normalized pipeline displacements for different landslide widths.

As depicted in Figure 9, the bottom line strains reach their maximum values in the middle of the pipe and minimum after the landslide area, while the top line strains display the reverse pattern. In the case of $B = 240$ m both top and bottom strains are tensile and coincide just after the landslide ($x/B = 0.5$). In the case of $B = 120$ m, although both bottom and top strains match quickly after the landslide, compressive strains appear in the middle of the pipeline and the end of the landslide zone along the top and the bottom line, respectively. Finally, in the case of $B = 60$ m, compressive strains increase rapidly along the top line of the pipeline. Although the total force applied to the pipeline is smaller, the situation created is more adverse than the previous two cases due to the local buckling phenomena.

4.3 Cross section dimensions

With respect to the influence of the diameter to thickness ratio (D/t) on the pipeline, three different ratios have been examined: $D/t = 15$, 30 and 45. Considering that the outer diameter

of the pipeline is constant and equal to 0.9144 m, larger D/t refers to smaller pipeline thickness. As shown in Figure 10, larger D/t ratio results in larger lateral normalized displacements, y/D , while the part of the pipeline moving laterally remains constant and it is 552 m in all cases. The absolute lateral movement of the pipeline is large in every case, and more specifically 30.7, 38.72 and 44.55 m for $D/t = 15, 30$ and 45, respectively.

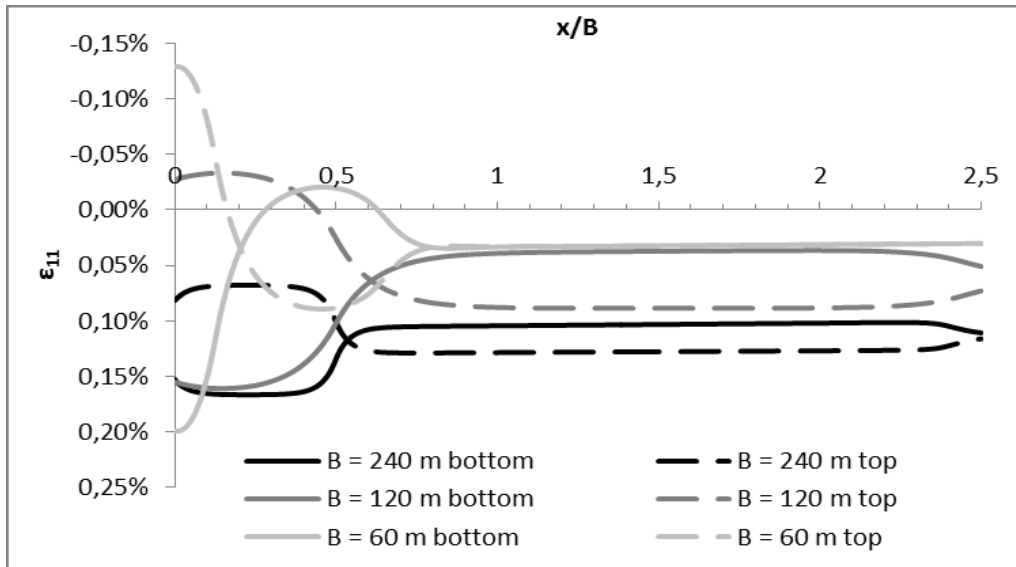


Figure 9: Comparison between axial strains for different landslide widths.

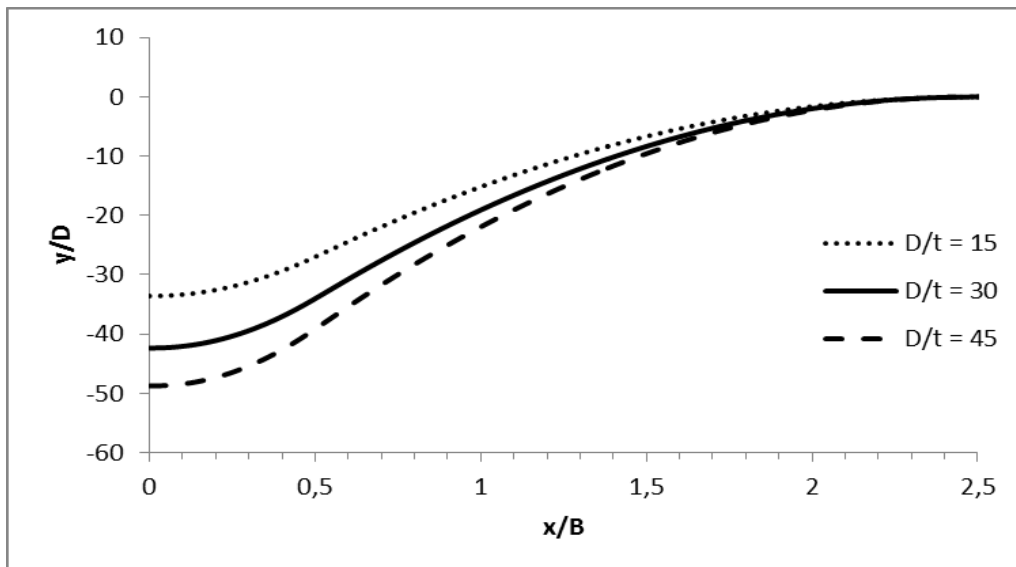


Figure 10: Comparison between normalized pipeline displacements for different cross sections.

As shown in Figure 11, the bottom line strains are maximum in the middle of the pipe and minimum after the landslide area, while the top line strains display the exact reverse pattern. For all cases considered, both top and bottom strains are tensile and coincide just after the landslide ($x/B = 0.5$). The only difference between the three cases is that the bigger the D/t ratio is the greater the tensile strains are; which can be directly attributed to the smaller cross section of the pipeline.

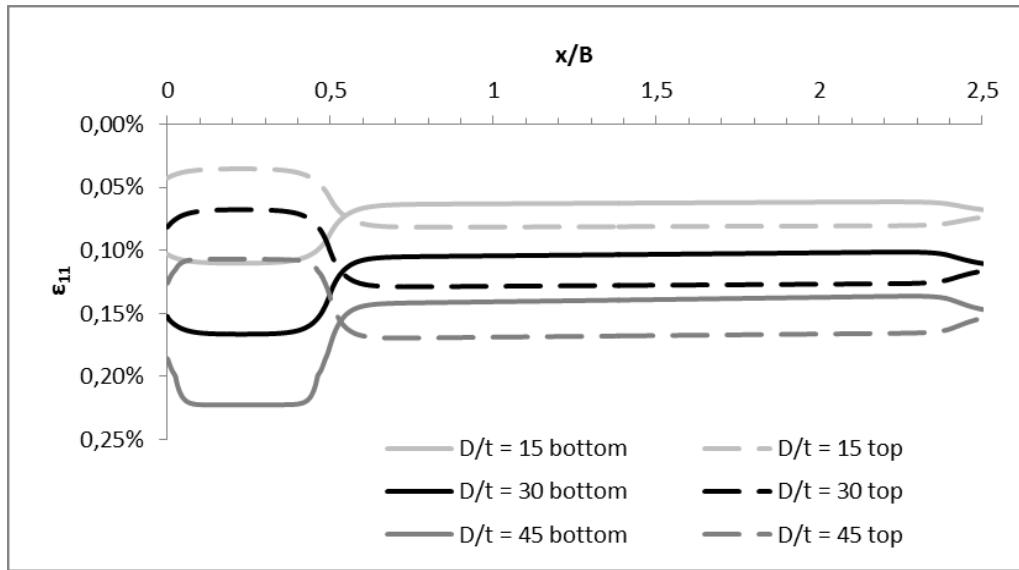


Figure 11: Comparison between axial strains for different cross sections.

4.4 Internal pressure levels

Regarding the influence of the internal pressure levels on the pipeline, three different pressures have been examined: $P_{in} = 0, 7.5$, and 15 MPa. As shown in Figure 12, greater internal pressure results in larger lateral normalized displacements, y/D , while the part of the pipeline moving laterally remains constant and it is 552 m in all cases. The absolute lateral movement of the pipeline is large in every case, and more specifically $36.56, 38.72$ and 37.64 m for $0, 7.5$ and 15 MPa internal pressure, respectively.

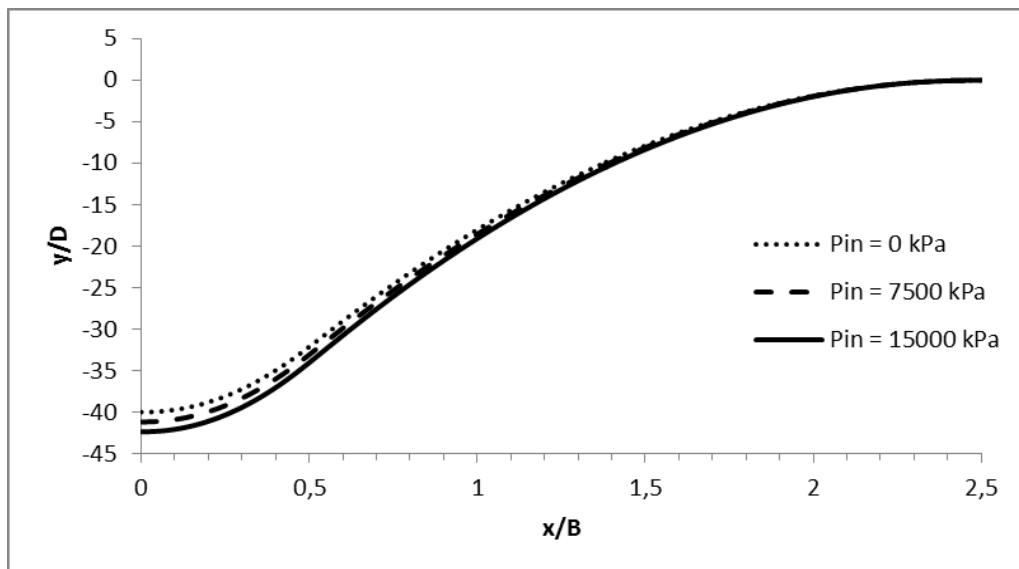


Figure 12: Comparison between normalized pipeline displacements for different internal pressures.

As shown in Figure 13, the bottom line strains are maximum in the middle of the pipe and minimum after the landslide area, while the top line strains display the exact reverse pattern. For all cases considered, both top and bottom strains are tensile and match just after the landslide ($x/B = 0.5$). The only difference between the three cases is that the bigger the internal

pressure is the greater the resulting tensile strains are; which is due to the fact that this is a more detrimental condition for the pipeline.

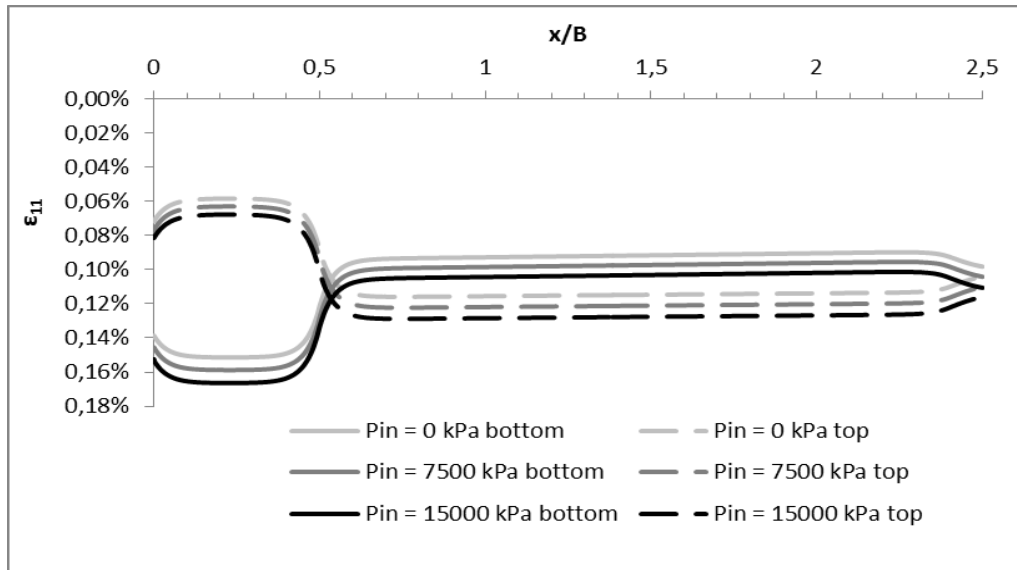


Figure 13: Comparison between axial strains for different internal pressures.

4.5 Bottom slope angle

Regarding the influence of bottom slope angle on the pipeline, three different angles have been examined: $\phi = 0^\circ$, 15° and 30° . In all cases, the slope angle is vertical to the pipeline axis. As shown in Figure 14, larger drag force results in larger lateral normalized displacements, y/D , and longer part of the pipeline moving laterally. It is noted that the absolute lateral movement of the pipeline is large in every case, and more specifically 38.72, 51.79 and 78.94 m for 0° , 15° and 30° degrees angle, respectively. Also, the length of the pipeline moving laterally is 552, 816 and 1440 m, for 0° , 15° and 30° , respectively.

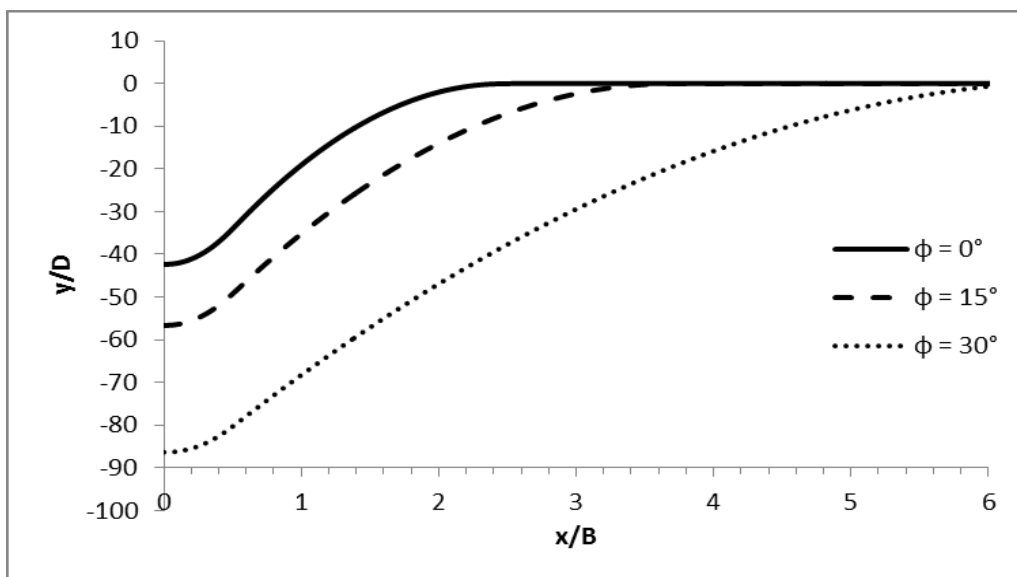


Figure 14: Comparison between normalized pipeline displacements for different slope angles.

As illustrated in Figure 15, the bottom line strains reach their maximum values in the middle of the geometry and minimum after the landslide area, while the top line strains display the exact reverse pattern. For all cases considered, both top and bottom strains are tensile and match just after the landslide ($x/B = 0.5$). The only difference between the three cases is that the steeper the slope angle is the greater the resulting tensile strains are, which can be explained by the increased distress of the pipeline.

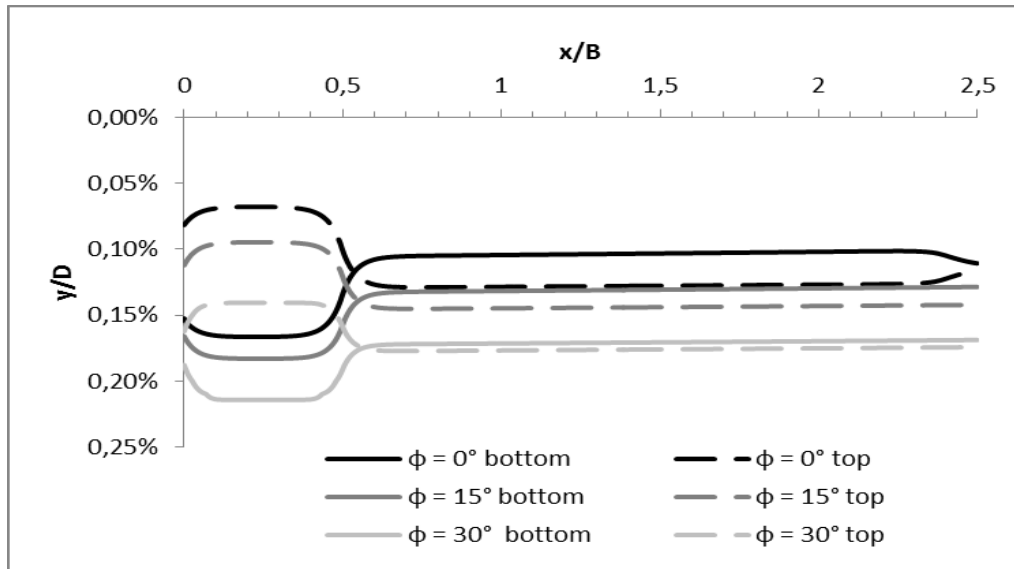


Figure 15: Comparison between axial strains for different slope angles.

5 CONCLUSIONS

The current work is an attempt to investigate the response of offshore pipelines subjected to lateral landslides. For this purpose, a computationally efficient numerical finite element model is developed and validated utilizing available numerical and analytical approaches. The fact that different numerical and analytical approaches result in similar pipeline response is promising. Nevertheless, validation against real pipe response or experimental results is always preferred, but very difficult due to lack of data.

The main findings of the parametric study can be summarized as follows:

- Regarding the pipeline lateral displacement, the parametric study indicates that larger drag force, landslide width, internal pressure and slope angle result in greater displacements. Furthermore, pipelines with thinner cross-section exhibit greater displacements.
- With respect to the part of the pipeline moving laterally, the parametric study indicates that larger greater landslide width and steeper slope angle result in longer part of the pipeline to be exposed to lateral movement. In all other cases the part of the pipeline moving laterally remains constant.
- Regarding the axial strains, it is concluded that bottom and top line strains display the exact reverse pattern. However, in almost every case strains remain tensile, which is beneficial since the pipeline has smaller resistance to compressive strains. Compressive strains appear only for small landslide widths and small drag forces, with the former being more critical. It is recommended to avoid areas with landslide zones having small width.

Further parametric investigation of the examined problem is needed. Other parameters, such as soil conditions, material properties, as well as non-symmetrical configurations should be investigated. Finally, the use of various mitigation measures should also be studied for the worst case scenarios, in order to ensure the safety and functionality of offshore pipelines in such adverse conditions.

REFERENCES

- [1] A. Zakeri, Review of state-of-the-art: Drag forces on submarine pipelines and piles caused by landslide or debris flow impact. *Journal of Offshore Mechanics and Arctic Engineering*, **131**(1), 014001, 2009.
- [2] A. Zakeri, K. Hoeg, F. Nadim, Submarine debris flow impact on pipelines–Part I: Experimental investigation. *Coastal Engineering*, **55**(12), 1209-1218, 2008.
- [3] A. Zakeri, K. Hoeg, F. Nadim, Submarine debris flow impact on pipelines–Part II: Numerical Analysis. *Coastal Engineering*, **56**(1), 1-10, 2009.
- [4] M.F. Randolph, D.J. White, Interaction forces between pipelines and submarine slides – A geotechnical viewpoint. *Ocean Engineering*, **48**, 32-37, 2012.
- [5] J. Liu, J. Tian, P. Yi, Impact forces of submarine landslides on offshore pipelines. *Ocean Engineering*, **95**, 116-127, 2015.
- [6] F. Sahdi, C. Gaudin, D.J. White, N. Boylan, M.F. Randolph, Centrifuge modelling of active slide–pipeline loading in soft clay. *Geotechnique*, **64**(1), 16–27, 2014.
- [7] D.A.S. Bruton, D.J. White, M. Carr, J.C.Y. Cheuk, Pipe-soil interaction during lateral buckling and pipeline walking-The safebuck jip. *Offshore Technology Conference*, Houston, TX, U.S.A, 2008.
- [8] D.J. White, C.Y. Cheuk, Modelling the soil resistance on seabed pipelines during large cycles of lateral movement. *Marine Structures*, **21**, 59-79, 2008.
- [9] M.F. Randolph, D. White, Y. Yan, Modelling the axial soil resistance on deep-water pipelines. *Geotechnique*, **62**, 9, 837-846, 2012.
- [10] J. Wang, Z. Yang, Axial friction response of full-scale pipes in soft clays. *Applied Ocean Research*, **59**, 10-23, 2016.
- [11] I. Guha, M.F. Randolph, D.J. White, Evaluation of elastic stiffness parameters for pipeline-soil interaction. *Journal of Geotechnical and Geoenvironmental Engineering*, **142**(6), 04016009, 2016.
- [12] E.J. Parker, C. Traverso, R. Moore, T. Evans, N. Usher), Evaluation of landslide Impact on Deepwater Submarine Pipelines. *Offshore Technology Conference*, Houston, Texas, U.S.A., May 5-8, 2008.
- [13] F. Yuan, L. Wang, R. Shi, A refined analytical model for landslide or debris flow impact on pipelines. Part I: Surface pipelines. *Applied Ocean Research*, **35**, 95-104, 2012a.
- [14] F. Yuan, L. Wang, R. Shi, A refined analytical model for landslide or debris flow impact on pipelines. Part II: Embedded pipelines. *Applied Ocean Research*, **35**, 105-114, 2012b.

- [15] F. Yuan, L. Li, Z. Guo, L. Wang,, Landslide impact on submarine pipelines: Analytical and numerical analysis. *Journal of Engineering Mechanics*, **141(2)**, 28-37, 2014.
- [16] L. Zhang, X. Zhao, X. Yan, X. Yang, A semi-analytical method of stress-strain analysis of buried steel pipelines under submarine landslides. *Applied Ocean Research*, **59**, 35-52, 2016.
- [17] D. Chatzidakis, Y. Tsompanakis, P.N. Psarropoulos, Efficient earthquake resistant design of natural gas pipelines subjected to large kinematic distress. *The Fifteenth International Conference on Civil, Structural and Environmental Engineering Computing*, Prague, Czech Republic, September 1-4, 2015
- [18] ABAQUS, (2014). ABAQUS/Analysis user's manual-version 6.14, Simulia Corp., Providence, RI, USA.
- [19] E.C. Ting, C. Shih, Y.K. Wang, Fundamentals of a vector form intrinsic finite element: Part I. Basic procedure and a plane frame element. *Journal of Mechanics*, **20(2)**, 113-122, 2004.
- [20] Trans Adriatic Pipeline – TAP, *Environmental and Social Impact Assessment (ESIA) Albania: Section 4 – Project Description*, Tirana, Albania, 2013.
- [21] American Society of Civil Engineers (ASCE), Federal Emergency Management Agency (FEMA), *American Lifelines Alliance – ALA, Guidelines for the design of buried pipe*, 2001.